

Thermodynamic Properties of Adsorbed Water on Silica Gel: Exergy Losses in Adiabatic Sorption Processes

W. M. Worek* and W. Zheng†

University of Illinois at Chicago, Chicago, Illinois 60680

and

J.-Y. Sant‡

National Chung-Hsing University, Taichung, Taiwan 400, Republic of China

In order to perform exergy analyses to optimize the transient heat and mass transfer processes involving sorption by solid adsorbents, the thermodynamic properties of adsorbed water must be determined. In this paper the integral enthalpy and entropy are determined directly from isotherm data of water adsorbed on silica gel particles and silica gel manufactured in the form of a felt with 25% cotton as a support and Teflon as a binder. These results are then used to evaluate the exergy losses, due to the sorption and the convective heat and mass transfer processes, that occur in each portion of an adiabatic desiccant dehumidification cycle.

Nomenclature

A_v	= heat transfer surface area per unit volume, m^2/m^3
b_{ij}	= coefficients of polynomial given in Eq. (2)
c_1	= specific heat of air, J/kg-K
c_w	= specific of the wall, J/kg-K
c_{wR}	= reference specific of the wall, J/kg-K
EX	= exergy flux, kW
f	= fraction of desiccant in the wall, kg desiccant/kg wall
h	= specific enthalpy, J/kg
h_1	= heat transfer coefficient, $\text{W/m}^2\text{-K}$
K	= conversion factor, no. of molecules- $\text{g}/\text{cm}^3\text{-m}^2$
K_y	= mass transfer coefficient, $\text{kg/m}^2\text{-s}$
M	= molecular weight of adsorbate, g/mole
\dot{m}_1	= mass flow rate of air, kg/s
m_w	= mass of the wall, kg
N	= Avogadro's constant, $6.02 \cdot (10^{23})$ molecules/mole
P	= vapor pressure, kPa
P_{sat}	= saturation pressure of water vapor in air, kPa
Q	= heat of sorption, $\text{kJ/kg H}_2\text{O}$
R	= gas constant of adsorbed molecules, J/kmole-K
S	= surface area of adsorbent, $\text{m}^2/\text{g silica gel}$
s	= specific entropy, kJ/kg-K
T, \bar{T}	= temperature and average temperature, K or $^{\circ}\text{C}$
T_0	= environmental temperature, K or $^{\circ}\text{C}$
T_1	= airstream temperature, $^{\circ}\text{C}$
t_A	= time, s
t_{AF}	= total time, s
V	= dehumidifier volume, m^3
v	= volume of adsorbed molecules (at STP, 0°C , and 101.325 kPa) per gram of adsorbent, $\text{cm}^3/\text{g silica gel}$
v_m	= monolayer capacity, $\text{cm}^3 \text{H}_2\text{O/g silica gel}$ or $\text{g H}_2\text{O/g silica gel}$
W	= moisture content, $\text{kg H}_2\text{O/kg silica gel}$
X	= nondimensional channel position, $VA_v h_1 x_A / (\dot{m}_1 c_1)$

XF	= nondimensional channel length, $VA_v h_1 x_{AF} / (\dot{m}_1 c_1)$
x	= relative pressure, P/P_{sat}
x_A	= dimensional channel position, m
x_{AF}	= total channel length, m
Y	= humidity ratio, $\text{kg H}_2\text{O/kg dry air}$
Γ	= number of adsorbed molecules per unit area, no. of molecules/ m^2
λ_1	= constant used in Eq. (15) = $K_y Q / h_1$
λ_2	= constant used in Eq. (14) = $K_y c_{wR} / (f h_1)$
λ_3	= constant used in Eq. (13), inverse of Lewis number = $K_y c_1 / h_1$
λ_4	= constant used in Eq. (15) = c_w / c_{wR}
Φ	= spreading pressure, J/m^2
ρ	= density, g/cm^3
ρ_{STP}	= density of adsorbate at STP, g/cm^3
τ	= nondimensional time, $VA_v h_1 t_A / (m_w c_{wR})$

Subscripts

f	= final
g	= water vapor
i	= initial
inlet	= inlet condition
L'	= saturated liquid state at T
s	= adsorbed state
w	= desiccant
0	= initial condition

Introduction

IN a physical adsorption process the thermodynamic properties of a solid adsorbent are unaltered by the sorbed molecules.¹ The sorbed molecules can then be considered as a simple substance in a potential field due to the solid adsorbent. Therefore, the thermodynamic properties of sorbed molecules (adsorbate), specifically the integral enthalpy and entropy of sorbed water, determined from experimental isotherms, can be used to evaluate exergy losses that occur during a sorption process.

Hill,^{1,2} Everett,³ and Honig⁴ derived relations to determine the thermodynamic properties of adsorbate. They showed that the entropy of an adsorbate and the heat of sorption can be related to other thermodynamic properties using the Clausius-Clapeyron equation.

Everett^{5,6} and Hill⁷⁻⁹ calculated the thermodynamic properties of sorbed molecules directly from statistical Brunauer-Emmett-Teller (BET) theory. They found the thermodynamic properties depend only on the ratio of the partition functions and the BET constant. These results are qualitatively similar in

Received Aug. 10, 1989; revision received Feb. 15, 1990. Copyright © 1990 by the American Institute of Aeronautics and Astronautics, Inc. All rights reserved.

*Associate Professor, Department of Mechanical Engineering (M/C 251), 900 Science and Engineering Offices, Box 4348.

†Research Engineer, Department of Mechanical Engineering.

‡Associate Professor, Department of Mechanical Engineering.

trend to those obtained using isotherm data. However, a comparison of the numerical values obtained using this approach with those obtained using isotherm data indicates that the numerical values obtained using the statistical BET theory are not reliable.

Hill et al.¹⁰ calculated entropies and heats of sorption for nitrogen sorbed on graphon using experimental isotherms. The thermodynamic properties were plotted vs the adsorbate surface coverage. These results showed the significance of the interfacial force (or potential field) that exists between the adsorbent and the adsorbate and the effect of the interfacial force on the thermodynamic properties of the sorbed molecules. Hill et al.¹⁰ also calculated the entropy that would be predicted using statistical BET theory. This yielded an entropy dependence on adsorbate surface coverage qualitatively similar to the one obtained previously. However, numerical values of the entropies were different. The numerical disagreement between the two methods occurred because of the assumptions made in the development of the BET theory. The most restrictive of these assumptions was the independence of the heat of sorption on adsorbate uptake. Therefore, BET theory generally cannot be used to accurately calculate the thermodynamic properties of an adsorbate.

Young and Crowell¹¹ have reviewed these methods, and a complete derivation of the thermodynamics of adsorption is given by Ruthven.¹²

In this work the internal enthalpy and entropy of bound water on two types of silica gel are determined from experimental isotherms. The thermodynamic properties of bound water on regular density silica gel particles are then used to calculate the exergy losses that occur in each portion of an adiabatic dehumidification process. This type of process occurs extensively in open-cycle desiccant dehumidification/cooling systems using solid desiccant dehumidifiers.¹³⁻¹⁶

Adsorption Isotherms

Two different groups of adsorption isotherm data are used in this work. One is for water vapor adsorbed on regular density silica gel particles, and the other is for water vapor adsorbed on a silica gel felt (2 mm thick) manufactured by a patented process.¹⁷

Regular Density Silica Gel Particles

Close and Banks¹⁸ plotted Hubard's equilibrium data¹⁹ for water vapor adsorbed by regular density silica gel on an Othmer chart. Jurinak²⁵ also curve-fitted Hubard's equilibrium data using the same approach and found a similar expression for the isotherm shape. The equilibrium equation used here is from Jurinak and has the following form:

$$x = [2.112W]^{1.0 + f(W)} [0.2951 P_{\text{sat}}]^{f(W)} \quad (1)$$

where

$$\log_{10}[P_{\text{sat}}/P_0] = -(az + bz^2 + cz^4)/[(T + 273.15)(1 + dz)]$$

$$F(W) = 0.2843 \exp(-10.28W)$$

$$P_0 = 22105.8$$

$$a = 3.2437814$$

$$b = 5.86826 \cdot 10^{-3}$$

$$c = 1.1702379 \cdot 10^{-8}$$

$$d = 2.1878462 \cdot 10^{-3}$$

$$z = 374.12 - T$$

Equation (1) is valid for relative pressures of 0–0.35 and temperatures of 4–93°C, where P_{sat} has the units of kPa, and

T is in degrees Celsius. The W can be converted to the volume of water adsorbed if this water was present in the gas phase at STP (i.e., 101.325 kPa, 273.15 K). Assuming that water vapor acts as an ideal gas at STP, this relationship is determined using the ideal gas equation of state and is given by the following relationship: $v = 1244W$.

Silica Gel Felt

Charoensupaya²⁰ measured the isotherm for water vapor adsorbed on a silica gel felt using 25% cotton as a support and Teflon as a binder. The experimental results were curve-fitted using a linear regression program covering a range of relative pressures from 0 to 1. The curve-fitted equilibrium equation consists of the following.

For $0 < x < 0.278$,

$$w = a_{00} + (a_{10} + a_{11}T + a_{13}T^3)x + (a_{20} + a_{21}T)x^2 + (a_{30} + a_{31}T)x^3 \quad (2a)$$

For $0.278 < x < 1$,

$$w = b_{00} + (b_{10} + b_{11}T + b_{12}T^2 + b_{13}T^3)x + (b_{20} + b_{22}T^2)x^2 + (b_{30} + b_{31}T + b_{33}T^3)x^3 \quad (2b)$$

where

$a_{00} = 0.2356942 (10^{-2})$	$b_{00} = 0.08940556$
$a_{10} = 0.9435188$	$b_{10} = -0.2229145$
$a_{11} = -0.01031031$	$b_{11} = -0.7511698 (10^{-2})$
$a_{13} = 0.1798803 (10^{-6})$	$b_{12} = 0.9748001 (10^{-4})$
$a_{20} = -4.233338$	$b_{13} = -0.4422159 (10^{-6})$
$a_{21} = 0.046356$	$b_{20} = 1.400644$
$a_{30} = 7.92862$	$b_{22} = -0.5166332 (10^{-4})$
$a_{31} = -0.0854038$	$b_{30} = -0.8828706$
	$b_{31} = 0.3508607 (10^{-2})$
	$b_{33} = 0.1500048 (10^{-6})$

Similarly, T in Eqs. (2a) and (2b) are in degrees Celsius.

Thermodynamics of Adsorption

Consider the adsorption process that occurs between moist air and silica gel. As the water vapor and adsorbed molecules reach equilibrium, the molar chemical potentials of water in these two phases will be equal. The amount of air adsorbed on silica gel is much less than that of water vapor, therefore, the effect of air can be neglected. Based on these conditions, the Gibbs's adsorption equation can be derived in the following form¹:

$$\left. \frac{\partial(\ln p)}{\partial T} \right|_* = \frac{(h_g - h_s)}{RT^2} \quad (3)$$

where g and s are the thermodynamic properties of water vapor and adsorbed molecules, respectively, and p is the equilibrium pressure of water vapor. The function Φ is the spreading pressure, which is related to the interfacial force between the adsorbed molecules and solid adsorbent. The spreading pressure can be expressed in terms of an integral along an isotherm as follows¹:

$$\Phi = RT \int_0^p \Gamma(p, T) d(\ln p) \quad (4)$$

where T is the equilibrium temperature in Kelvin.

Equations (3) and (4) can be expressed in terms of relative pressure x by assuming that water vapor behaves as an ideal gas and the vapor phase enthalpy is only a function of temperature. Using this assumption, the Clapeyron equation can be applied to the process along a saturation line between the

vapor and liquid phases. Therefore, Eqs. (3) and (4) can be rearranged into the following form¹:

$$\left. \frac{\partial(\ln x)}{\partial T} \right|_* = \frac{(h_{L'} - h_s)}{RT^2} \quad (5)$$

and

$$\Phi = KRT \int_0^x \nu d(\ln x) \quad (6)$$

where the relation $\Gamma = K\nu$ has been introduced into Eq. (4), and K is given by Eq. (7):

$$K = \rho_{STP} N / (MS) \quad (7)$$

The subscript L' indicates the properties of saturated liquid water at the same T as the adsorbed molecules.

The spreading pressure is evaluated by using Eq. (6) with experimental isotherms. It is desirable to curve-fit experimental isotherms having the equilibrium moisture content equal to zero at zero relative pressure (i.e., $x = 0$). However, if the experimental isotherms are not curve-fitted in this manner, the spreading pressure can be evaluated by dividing the integration into two separate parts. At low relative pressure, the equilibrium isotherm is assumed to be a straight line (i.e., $\nu = ax$ for $0 < x < x_1$ or $0 < \nu < \nu_1$). At higher relative pressures (i.e., $x > x_1$ or $\nu > \nu_1$), a curve-fit of the experimental data available in this range is used. Using this approach, Eq. (6) can be expressed as follows:

$$\Phi(x, T) / [KR] = T \left[\nu_1 + \int_{x_1}^x \nu d(\ln x) \right] \quad (8a)$$

or

$$\Phi(x, T) / [KR] = T \left[\nu_1 + (\nu \ln x - \nu_1 \ln x_1) - \int_{\nu_1}^{\nu} \ln x d\nu \right] \quad (8b)$$

For a convenient value of spreading pressure the enthalpy difference can be calculated using the data at the corresponding states on two neighboring isotherms. The equation used in calculation is given as follows:

$$h_{L'} - h_s = R(\ln x_2 - \ln x_1) / (1/T_1 - 1/T_2) \quad (9)$$

The enthalpy difference, $(h_L - h_s)$, as suggested by Hill et al.,¹⁰ corresponds to an average relative pressure and temperature. Individually, these can be expressed as follows:

$$1/\bar{T} = (1/T_1 + 1/T_2)/2 \quad (10)$$

$$\ln \bar{x} = (\ln x_1 + \ln x_2)/2 \quad (11)$$

The relation between the integral entropy and enthalpy is obtained from the condition of equilibrium. That is, the molar chemical potentials are the same in both phases. This yields the relation, $h_s - h_g = T(s_s - s_g)$ for water vapor and adsorbed molecules in equilibrium. Using the equation of state for an ideal gas and the latent heat relation in a normal evaporation-condensation process for liquid, the following equation can be used to calculate the integral entropy of adsorbed molecules:

$$s_s - s_{L'} = (h_s - h_{L'}) / \bar{T} - R \ln \bar{x} \quad (12)$$

where $s_{L'}$ is the entropy of saturated liquid water. Its numerical value is given in the steam tables for a wide range of temperatures.

Using Eq. (8a) or (8b), two values, $\Phi_1/[KR]$ and $\Phi_2/[KR]$, were determined at isotherms corresponding to T_1 and T_2 ,

where $(T_2 - T_1) = 0.002^\circ\text{C}$. Then, by fixing x_1 , corresponding to the isotherm at T_1 , x_2 , which corresponds to the isotherm at T_2 , is determined so that the two values of $\Phi/[KR]$ are equal. Using Eqs. (10) and (11), \bar{T} and \bar{x} are evaluated. The integral enthalpy and entropy differences are calculated using Eqs. (9) and (12) and are considered as the properties of state (\bar{T}, \bar{x}) .

Using this approach, the integral enthalpy and entropy of the regular density silica particles and the silica gel felt were determined as a function of loading. These results are presented in Figs. 1-4. Figures 1 and 2 show that, for the silica gel particles, the integral enthalpy and entropy decrease with increasing loading. This occurs because, at high adsorbate uptakes, the sorbed water becomes more liquid-like in nature. If the desiccant were capable of adsorbing an infinite number of adsorbate layers, both the integral enthalpy and entropy

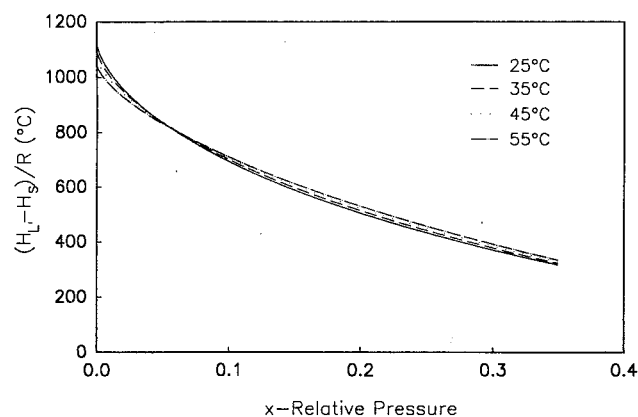


Fig. 1 Enthalpy difference of bound water adsorbed on the regular density silica gel particles.

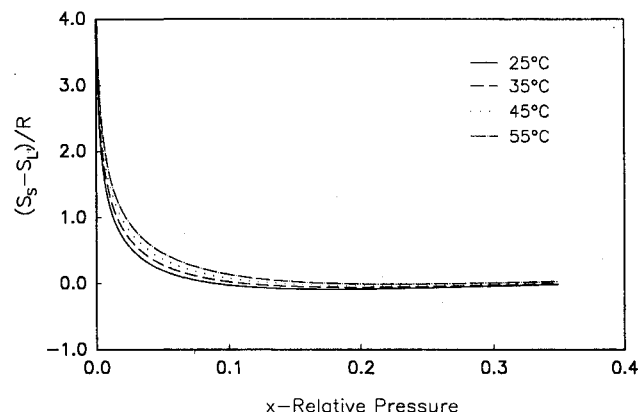


Fig. 2 Entropy difference of bound water adsorbed on the regular density silica gel particles.

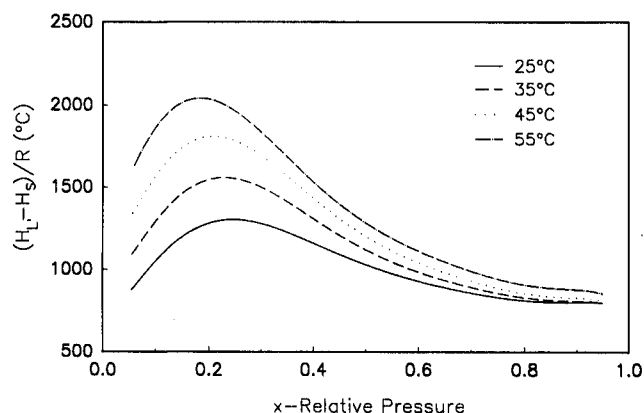


Fig. 3 Enthalpy difference of bound water adsorbed on the silica gel felt.

Table 1 Comparison of three different numerical methods for predicting the outlet states in an adiabatic dehumidification process

	Present paper finite-difference method		Maclaine-Cross finite-difference method ²²		Nonlinear analogy method ²⁵	
Conditions	$T, ^\circ\text{C}$	$Y, \text{g/kg}$	$T, ^\circ\text{C}$	$Y, \text{g/kg}$	$T, ^\circ\text{C}$	$Y, \text{g/kg}$
1) $x_{AF} = 2.5$ $t_F = 5.0$	57.396	9.752	57.305	9.759	57.971	9.076
2) $x_{AF} = 2.5$ $t_F = 10.0$	55.869	8.783	55.783	8.859	56.501	8.050
3) $x_{AF} = 10.0$ $t_F = 20.0$	67.001	6.814	66.726	6.745	67.059	6.360

Inlet state of the process stream: 35°C, 14.2 g/kg.

Inlet state of the regenerating stream: 85°C, 14.2 g/kg.

Table 2 Air states for an adiabatic rotary desiccant cooling system with purging

States	Temperature $T, ^\circ\text{C}$	Humidity ratio $Y, \text{g/kg}$	Mass flow rate $m_1, \text{kg/s}$
1	35.0	14.2	0.411
2	64.97	5.5	0.411
3	21.7	5.5	0.411
4	13.05	9.0	0.411
5	26.0	11.2	0.411
6	19.42	13.9	0.411
7	62.7	13.9	0.411
8	85.0	13.9	0.411
9	50.15	22.7	0.411
10	35.0	14.2	0.041
11	83.93	12.9	0.041

would approach zero. Figures 3 and 4 show the integral enthalpy and entropy for the silica gel felt. These results have considerably different shape compared to the results obtained for the silica gel particles. This difference is primarily due to the silica gel felts having a different desiccant as the base material (i.e., Syloid 63 vs regular density silica gel). Results having shapes similar to those presented in Figs. 3 and 4 have been published for different adsorbent-adsorbate pairs.¹²

The results of this analysis were also compared to a procedure given by Van den Bulck et al.²¹ This approach requires a two-step procedure where the equilibrium data are first plotted in an Othmer chart to determine the heat of sorption, and the ratio of the heat of sorption to the latent heat of vaporization is then curve-fitted with an expression that depends on the equilibrium moisture content of the material. This curve-fit is used to integrate and determine the integral enthalpy and entropy results. This method is to be contrasted with the method given in the present paper, where the isotherm data are used to directly determine the integral enthalpy and entropy and then these results are used to determine the heat of sorption without using the Othmer chart. Results of this comparison show a 1% agreement between the two methods.

Numerical Example: Rotary Desiccant Dehumidifier

Several authors²²⁻²⁵ have derived the governing equations for the process of heat and mass transfer in an adiabatic dehumidifier, which is a component of an open-cycle desiccant cooling system shown in Fig. 5. Assuming the overall Lewis number is equal to unity, the convective mass transfer coefficients thus can be substituted by the ratio of the convective heat transfer coefficient to the specific heat of the moist air. In doing so, the four governing differential equations for the process of heat and mass transfer in a solid desiccant dehumidifier consisting of many channels, where a typical channel is shown in Fig. 6, can be simplified to yield the following equations:

$$\frac{\partial Y}{\partial X} = \lambda_3(Y_w - Y) \quad (13)$$

$$\frac{\partial W}{\partial \tau} = \lambda_2(Y - Y_w) \quad (14)$$

$$\frac{\lambda_4 \partial T_w}{\partial \tau} = (T_1 - T_w) + \lambda_1(Y - Y_w) \quad (15)$$

$$\frac{\partial T_1}{\partial X} = (T_w - T_1) \quad (16)$$

subject to the following boundary and initial conditions:

$$Y = Y_{\text{inlet}} \quad \text{and} \quad T_1 = T_{\text{inlet}} \quad \text{at} \quad X = 0$$

$$T_w = T_{w0}(X) \quad \text{and} \quad W = W_0(X) \quad \text{at} \quad \tau = 0$$

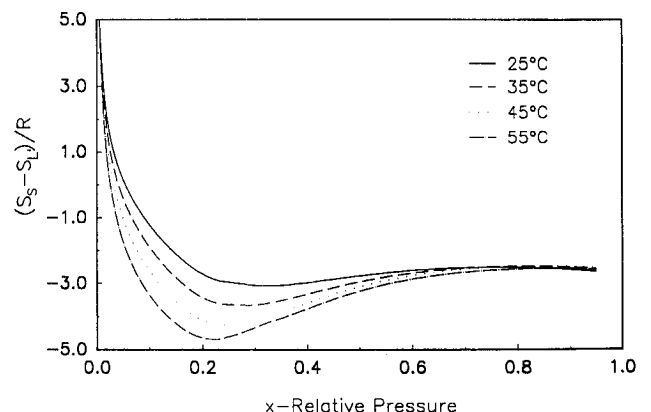
and the equilibrium equation used in the simulation is Eq. (1).

Equations (13-16) have been solved using an explicit finite-difference scheme²³ for a fixed-bed system under periodic, steady-state operation. Jurinak²⁵ compared the numerical results obtained using three different numerical approaches that solved the process of heat and mass transfer in a rotary dehumidifier. The three approaches were the Maclaine-Cross, finite-difference method,^{22,24} the nonlinear analogy method, and the intersection point method. The results of Jurinak's comparison showed that the predictions of the three methods agree. Using Jurinak's test case, several computer runs were performed to compare the present model to the Maclaine-Cross model and the nonlinear analogy method. The results of the comparison, listed in Table 1, also show a good agreement between the present model and the other two models.

Using the standard indoor and outdoor conditions of the American Refrigeration Institute as the input data (i.e., outdoor temperature 35°C, outdoor humidity ratio 0.0142 kg H₂O/kg dry air, indoor temperature 26.7°C, and indoor humidity ratio 0.0112 kg H₂O/kg dry air), a nominal rotary solid desiccant dehumidifier, including a purging mode, is simulated for X_f and τ of 15 and 40, respectively, and with a desiccant mass fraction of 50%. In the calculation the purging period is selected as 5% of the entire sorption period. Table 2 gives the thermodynamic states in the desiccant cooling system, operating in the ventilation mode, which includes the states entering and leaving the dehumidifier. Table 3 summarizes the average thermodynamic state of the dehumidifier matrix, the temperature, and the bound water content (desiccant moisture content), at the end of each process.

Since the initial and final states of the bound water for the adsorption, purging, and desorption processes are not the same, the change of entropy in the dehumidifier has to be taken into account when determining the exergy losses. Therefore, the exergy losses in a dehumidifier for each of the three different operating modes are evaluated using the following equation:

$$(EX)/\dot{m}_1 t_{AF} = T_0(s_2 - s_1) + (m_w/\dot{m}_1 t_{AF})T_0[W_f s_f - W_i s_i] \\ + (m_w/\dot{m}_1 t_{AF})c_w T_0 \ln(T_{w,f}/T_{w,i}) \quad (17)$$

**Fig. 4 Entropy difference of bound water adsorbed on the silica gel felt.**

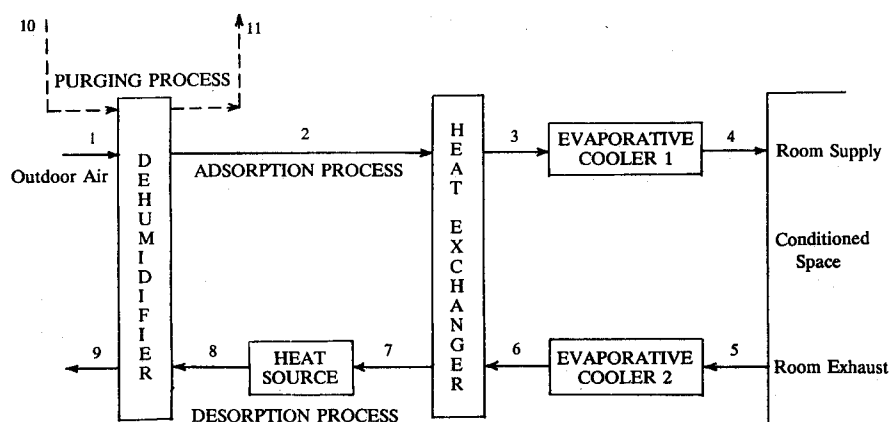


Fig. 5 Adiabatic solid desiccant dehumidifier.

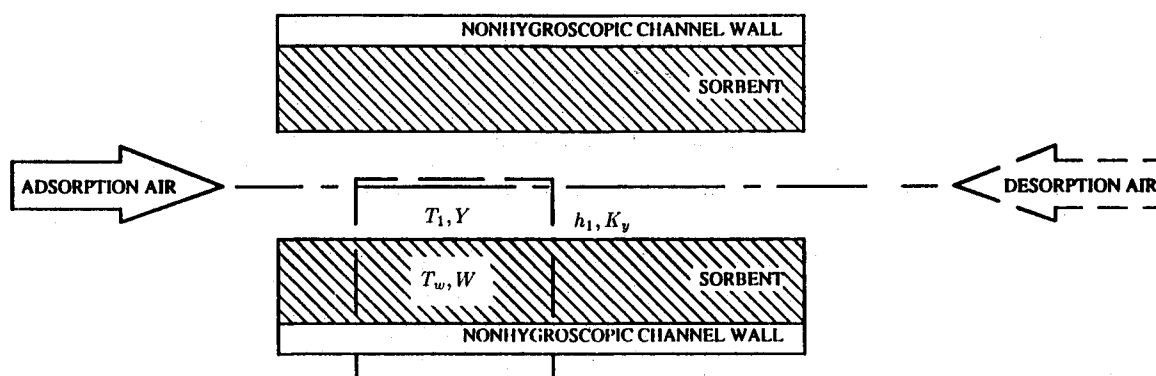


Fig. 6 Typical adiabatic solid desiccant dehumidifier channel.

Table 3 Average bound water states at the end of each node

	Average desiccant temperature $T, ^\circ\text{C}$	Average desiccant moisture content $W, \text{ kg H}_2\text{O/kg desiccant}$
Desorption	76.9	0.0368
Purging	65.8	0.0375
Adsorption	48.0	0.0825

Table 4 Exergy loss in each mode of the dehumidification cycle

	Air-water vapor mixture	Bound water	Solid adsorbent	Total exergy loss
Desorption	- 8.524	- 0.613	9.485	0.348
Purging	4.448	- 0.298	- 3.607	0.543
Adsorption	5.016	0.911	- 5.878	0.049
Net	0.940	0.000	0.000	0.940

All values are based on average properties and are given in kJ/kg dry air.

Equation (17) represents the net exergy loss in a process where the average initial and final thermodynamic states of the solid (i and f , respectively) are determined from the average wall temperature and the average desiccant moisture content. The first term on the right side of Eq. (17) is due to the entropy change in the moist air; the second term represents the bound water effect; and the last term is due to the entropy change in the solid that is due only to the change in temperature.

Table 4 lists the exergy loss in each mode. The results are based on a kilogram of air passing through a single dehumidifier channel and take into account the change in temperature and moisture content of the airstreams and the desiccant material. The change in entropy of the desiccant material is evaluated using Table 3. The second line in Table 4 indicates the exergy loss in the purging mode, which is time-weighted in

order to have the same basis as those results in the sorption mode. These results show that the purging and desorption modes have the largest exergy losses. The fact that the purging portion of the cycle has the largest exergy loss is expected, since, in the purging process, air from the adsorption process is being used to precool the adsorbent before beginning the adsorption process and is discarded to the atmosphere. The exergy loss in the desorption portion of the cycle is also high due to the relatively high desorption temperatures (compared to the adsorption process). The accuracy in which the exergy of bound water is determined is important. Inaccuracies in calculating these values would give erroneous exergy losses in a portion of dehumidification cycle or, in general, any process where the initial thermodynamic state of the adsorbent is different than the final state.

Conclusions

The method of calculating the integral enthalpy and entropy of water adsorbed on a solid adsorbent is presented. Using this procedure the integral enthalpy and entropy of water adsorbed on two desiccant samples are determined without use of an Othmer chart. These samples are pure silica gel particles and a desiccant felt. The results show that the integral enthalpy and entropy can vary substantially for different materials.

The integral entropy values for the silica gel particles were then used to calculate the exergy losses in each portion of an adiabatic dehumidification cycle to illustrate the use of results. The exergy of bound water or any adsorbate must be known when calculating the exergy loss for a process where the initial and final state of the adsorbent material are different.

References

- Hill, T. L., "Statistical Mechanics of Adsorption. V. Thermodynamics and Heat of Adsorption," *Journal of Chemical Physics*, Vol. 17, No. 6, 1949, pp. 520-535.
- Hill, T. L., "Thermodynamics Transition from Adsorption to So-

lution," *Journal of Chemical Physics*, Vol. 17, No. 5, 1949, pp. 503-507.

³Everett, D. H., "Thermodynamics of Adsorption. Part 1.—General Consideration," *Transactions of the Faraday Society*, Vol. 46, 1950, pp. 453-459.

⁴Honig, J. M., "Systematization of the Thermodynamics of Gas Adsorption Phenomena," *Journal of Colloid and Interface Science*, Vol. 70, No. 1, 1979, pp. 83-89.

⁵Everett, D. H., "The Thermodynamics of Adsorption. Part 2.—Thermodynamics of Monolayers on Solids," *Transactions of the Faraday Society*, Vol. 46, 1950, pp. 942-957.

⁶Everett, D. H., "The Thermodynamics of Adsorption. Part 3.—Analysis and Discussion of Experimental Data," *Transactions of the Faraday Society*, Vol. 46, 1950, pp. 957-969.

⁷Hill, T. L., "Statistical Mechanics of Adsorption. VII. Thermodynamic Functions for the B.E.T. Theory," *Journal of Chemical Physics*, Vol. 17, No. 9, 1949, pp. 772-774.

⁸Hill, T. L., "Statistical Mechanics of Multimolecular Adsorption. I," *Journal of Chemical Physics*, Vol. 14, No. 4, 1946, pp. 263-267.

⁹Hill, T. L., "Statistical Mechanics of Multimolecular Adsorption. II. Localized and Mobile Adsorption and Absorption," *Journal of Chemical Physics*, Vol. 14, No. 7, 1946, pp. 263-267.

¹⁰Hill, T. L., Emmett, P. H., and Joyner, L. G., "Calculation of Thermodynamic Functions of Adsorbed Molecules from Adsorption Isotherm Measurements: Nitrogen on Graphon," *Journal of the American Chemical Society*, Vol. 73, 1951, pp. 5102-5107.

¹¹Young, D. M., and Crowell, A. D., *Physical Adsorption of Gases*, Butterworths, London, 1962.

¹²Ruthven, D. M., *Principles of Adsorption and Adsorption Processes*, Wiley, New York, 1984.

¹³Pennington, N. A., "Humidity Changer for Air-Conditioning," U.S. Patent No. 2,700,537, 1955.

¹⁴Dunkle, R. V., "A Method of Solar Air-Conditioning," *Mechanical and Chemical Engineering Transactions*, Vol. 73, 1965, pp. 73-78.

¹⁵Banks, P. J., Close, D. J., and Maclaine-Cross, I. L., "Coupled

Heat and Mass Transfer on Fluid Flow through Porous Media," *Heat Transfer*, VII-CT3.1, Elsevier Publishing Co., Amsterdam, The Netherlands, 1970, pp. 1-10.

¹⁶Dini, S. and Worek, W. M., "Sorption Equilibrium of a Solid Desiccant Felt and the Effect of Sorption Properties on Cooled-Bed Desiccant Cooling System," *Heat Recovery Systems*, Vol. 6, No. 2, 1986, pp. 151-167.

¹⁷Gidaspow, D., Lavan, Z., and Onischak, M., "Thermally Regenerative Desiccant Element," U.S. Patent No. 4,341,539, 1982.

¹⁸Close, D. J., and Banks P. J., "Coupled Equilibrium Heat and Single Adsorbate Transfer in Fluid Flow Through a Porous Medium—II. Predictions for a Silica-Gel Air-Drier Using Characteristics Chart," *Chemical Engineering Science*, Vol. 27, No. 2, 1972, pp. 1157-1169.

¹⁹Hubard, S. S., "Equilibrium Data for Silica Gel and Water Vapor," *Industrial and Engineering Chemistry*, Vol. 46, No. 2, 1954, pp. 356-358.

²⁰Charoensupaya, D., "Experimental and Analytic Investigations of Composite Desiccant Structure and Low Humidity Adsorption," Ph.D. Dissertation, Illinois Inst. of Technology, Chicago, 1986.

²¹Van den Bulck, E., Klein, S. A., and Mitchell, J. W., "Second Law Analysis of Solid Desiccant Rotary Dehumidifiers," *Journal of Solar Energy Engineering*, Vol. 110, No. 1, 1988, pp. 2-9.

²²Maclaine-Cross, I. L., "A Theory of Combined Heat and Mass Transfer in Regenerators," Ph.D. Dissertation, Dept. of Mechanical Engineering, Monash University, Melbourne, Australia, 1974.

²³Mathiprakasam, B., "Performance Predictions of Silica Gel Desiccant Systems," Ph.D. Dissertation, Illinois Inst. of Technology, Chicago, 1979.

²⁴Brandemuehl, M. J., "Analysis of Heat and Mass Regenerators with Time Varying or Spatially Nonuniform Inlet Conditions," Ph.D. Dissertation, Univ. of Wisconsin-Madison, 1982.

²⁵Jurinak, J. J., "Open-Cycle Solid Desiccant Cooling—Component Models and System Simulation," Ph.D. Dissertation, Univ. of Wisconsin-Madison, 1982.

Recommended Reading from the AIAA Progress in Astronautics and Aeronautics Series . . .



Thermal Design of Aeroassisted Orbital Transfer Vehicles

H. F. Nelson, editor

Underscoring the importance of sound thermophysical knowledge in spacecraft design, this volume emphasizes effective use of numerical analysis and presents recent advances and current thinking about the design of aeroassisted orbital transfer vehicles (AOTVs). Its 22 chapters cover flow field analysis, trajectories (including impact of atmospheric uncertainties and viscous interaction effects), thermal protection, and surface effects such as temperature-dependent reaction rate expressions for oxygen recombination; surface-ship equations for low-Reynolds-number multicomponent air flow, rate chemistry in flight regimes, and noncatalytic surfaces for metallic heat shields.

TO ORDER: Write, Phone or FAX:

American Institute of Aeronautics and Astronautics,
c/o TASCOT, 9 Jay Gould Ct., P.O. Box 753, Waldorf, MD 20604
Phone (301) 645-5643, Dept. 415 ■ FAX (301) 843-0159

Sales Tax: CA residents, 7%; DC, 6%. For shipping and handling add \$4.75 for 1-4 books (call for rates for higher quantities). Orders under \$50.00 must be prepaid. Foreign orders must be prepaid. Please allow 4 weeks for delivery. Prices are subject to change without notice. Returns will be accepted within 15 days.

1985 566 pp., illus. Hardback

ISBN 0-915928-94-9

AIAA Members \$54.95

Nonmembers \$81.95

Order Number V-96